Transactions of NAMP 20 (2024) 31-44

Transactions of
The Nigerian Association of
Mathematical Physics
Journal homepage: https://nampjournals.org.ng

Utilizing GIS, RS, and AHP Methodologies for Adaptive Flood Risk Mapping in Ovia-North East Local Government Area, Edo State, Nigeria.

[1]Ilaboya, I.R., [2]Okonkwo, N.H., [3]Nwanchukwu, S, and [4]Ilaboya, I.A

[1,3,4]Department of Civil Engineering, Faculty of Engineering, University of Benin, Benin City, Edo State, Nigeria
[2]Department of Industrial Safety and Environmental Technology (ISET), Petroleum Training Institute, Effurun, Delta State, Nigeria

ARTICLE INFO

Article history:
Received xxxxx
Revised xxxxx
Accepted xxxxx
Available online xxxxx

Keywords:
Flood risk,
Multi-Criteria Analysis,
Geographic Information System,
Analytical Hierarchy Process.

ABSTRACT

Flooding due to excessive rainfall is a frequent and widely reported disaster. This study aims to create flood risk maps for public use and estimate the likelihood of flooding in rapidly urbanizing areas. An integrated Analytical Hierarchy Process (AHP) and Geographic Information System (GIS) approach was used to model flood risk zones. A spatial decision support system analyzed flood risks, utilizing datasets such as high-resolution satellite images, SRTM DEM data, FAO soil data, and rainfall data. Flood-enhancing elements, including vulnerability mapping, were created in GIS at a 1: 400,000 scale. This multi-parametric approach considered factors such as rainfall distribution, elevation, slope, drainage network, land use, and soil type. The output raster maps were ranked using the Weighted Linear Combination method and analyzed via Multi-Criteria Analysis (MCA), with a consistency ratio of 0.037 confirming the model's validity. The study identified topography and rainfall as significant contributors to flood risk

1. Introduction

As climate change intensifies, the frequency and intensity of natural disasters, particularly floods, pose a growing threat to vulnerable regions worldwide. In the quest for proactive and effective disaster management, the amalgamation of cutting-edge technologies has become imperative.
Since the dawn of civilization, people have been subject to devastating natural disasters such as floods, landslides, earthquakes, cyclones, etc. [1,2,3]. The severity and frequency of all-natural risks and disasters have grown significantly over time, with a variety of contributing variables [4]. Physical forces and human activity have speed up this process, endangering the ecosystem and the environment on a large scale [4,2].

*Corresponding author: Ilaboya, I.R.
E-mail address: rudolph.ilaboya@uniben.edu
https://doi.org/10.60787/tnamp.v20.381

Floods are the most frequent hydrometeorological catastrophe occurrence among natural disasters, posing a significant risk to social, economic, and physical aspects [5,6]. From 1996 to 2015, around 150,061 flood events occurred in the world and were responsible for 11.1% of the global disaster fatalities, based on information from the United Nations Office for Disaster Risk Reduction (UNISDR) [7,8]. Flooding is a serious disaster that has caused economic damage and loss of human life throughout history. However, the long-term secondary effect of a flood disaster is more severe, including economic losses as well as impacts like disease and malnutrition in the impacted communities [9,10,11].

A significant increase in floods around the world has been observed in recent years. Not only have the frequency of flood increased, there is also an unusual increase in the severity of floods [12,13]. Though floods cannot be entirely prevented, appropriate planning and protection measures helps in the reduction of the severity of floods and the damages they cause [14,15,16]. The increasing rate of flooding in recent time can be linked to the problem of ongoing climate change; which is a result of greenhouse gas emissions contributing to global warming and is further exacerbated by changes in land use brought on by human activity, extreme weather, and hydrometeorological events [12,17, 18, 19]

Researchers from all over the world have clamoured for early warning signals that will aid with flood preparedness and prevention due to the danger that floods and other water related disasters pose. One of the most crucial components of early warning systems or strategies for the prevention and mitigation of future flood situations is the mapping and analysis of flood vulnerability because it identifies the most vulnerable areas based on physical factors that determine the propensity for flooding [20, 21, 22].

The word "vulnerability" refers to an evaluation of possible risk that takes into account a person's socioeconomic capacity to deal with the worst-case scenario following a catastrophic catastrophe. Determine the likelihood and severity of the flood danger occurring over an extended period of time is the goal of the flood vulnerability assessment [23, 24, 25]. According to [26], the vulnerability assessment sought to ascertain the likelihood over the long horizons of decades to support the risk management operations.

The conventional paradigm of flood hazard assessment often falls short in providing the depth and precision required for strategic planning and mitigation efforts. This study breaks new ground by integrating GIS for spatial analysis, RS for comprehensive data acquisition and AHP for robust decision-making, offering a groundbreaking methodology for flood hazard mapping. The confluence of these technologies not only enhances the accuracy of hazard identification but also provides a holistic understanding of the dynamic factors contributing to flood vulnerability. What sets this research apart is its focus on the Ovia-North East Local Government Area, an area with its unique topographical and climatic characteristics. By tailoring the methodology to the specific context of this region, our study aims to deliver insights that are not only academically rigorous but also directly applicable to the challenges faced by the local community. This localized approach underscores the novelty of our research, as it bridges the gap between advanced technological applications and the practical needs of a specific geographic area.

2. Research Methodology

2.1 Description of study area

The study area, Ovia North-East Local Government Area, is situated in Edo State, which is part of Nigeria's South-South geopolitical zone. Its headquarters is located in the town of Okada. It consists of a number of settlements spread over the latitudes of 5° and 7° 40' N and 5° and 6° 30' E. The region is 2,301 km^2 in area. It is a tropical rainforest area that gets a lot of rain. As of 2006, 153,849 people lived in Ovia North-East (National Population Census, 2006). A significant river,

the Ovia River, which runs through each community in the LGA, effectively drains the city. The study area map is presented in Figure 1

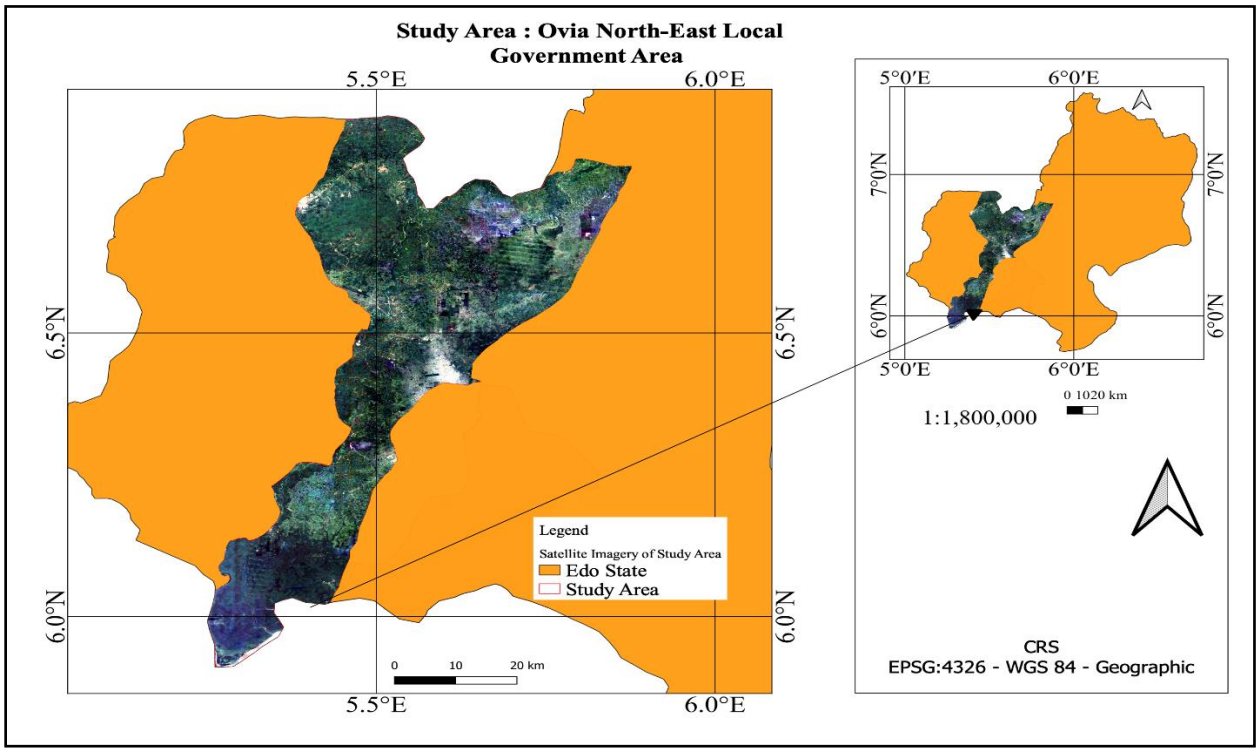

Figure 1: Study area map.

2.2 Data Requirement

Both remotely sensed data and field data were collected for this study. Table 1 shows the data type, source and year.

Table 1: List of data required for the study

S/n	Data / Scale	Type	Source /Date
1.	Landsat 8 Satellite imagery (30m Resolution)	Remotely sensed	USGS (2022)
2.	SRTM Data (30m DEM Resolution)	Remotely sensed	USGS (2022)
3.	Topographical map 1:100,000	Digital Copy	Federal Survey (2018)
4.	Geological Map (1:500,000)	Digital copy	Nigerian Geological survey Agency (2018)
5.	FAO Soil Data	Remotely Sensed	FAO (2022)
6.	Rainfall Data	40 years Annual Data	1982– 2022

2.3 Data Acquisition

2.3.1 Landsat 8 Data

The Landsat 8 data products were downloaded from USGS EROS Center, the downloaded image was processed and imported to Arcmap Software environment. Landsat Program has provided over 40 years of calibrated medium spatial resolution data of the Earth's surface to a broad and varied user community. Landsat 8 is the latest in a continuous series of land remote sensing satellites.

2.3.2 Shuttle Radar Topographic Mission (SRTM 30m Resolution)

The NASA Shuttle Radar Topographic Mission (SRTM) has provided digital elevation data (DEMs) for over 80% of the globe. The data was acquired via download from the USGS EROS Center.

2.3.3 Topographical and Geological Maps

Topographical Map and Geological map was acquired from the office of the surveyor general and Nigerian geological survey agency respectively.

2.3.4 World Soil Geodatabase

The Food and Agricultural Organization (FAO) has provided digital soil data for over 80% of the globe. The data was acquired via download from the FAO website

2.4 Satellite Data processing

i. All acquired satellite imageries were projected to the UTM coordinate system (WGS84 UTM32N)
ii. Also, all hard copy maps were scanned and geo-referenced to the UTM coordinate system (WGS84 UTM32N)
iii. Using a specified boundary extent as the "Area of interest "all acquired data were clipped using the Clip tool in the Arcmap Environment to the specified Area of interest.

2.5 Generation of Flood Thematic Maps

The thematic data which include; precipitation, drainage density, topography, slope, soil and land use land cover, were generated in raster format using ArcGIS version 10.6.1. The step-by-step methodology employed to generate the various raster data is shown in the schematics presented in Figures 2 – 6 respectively.

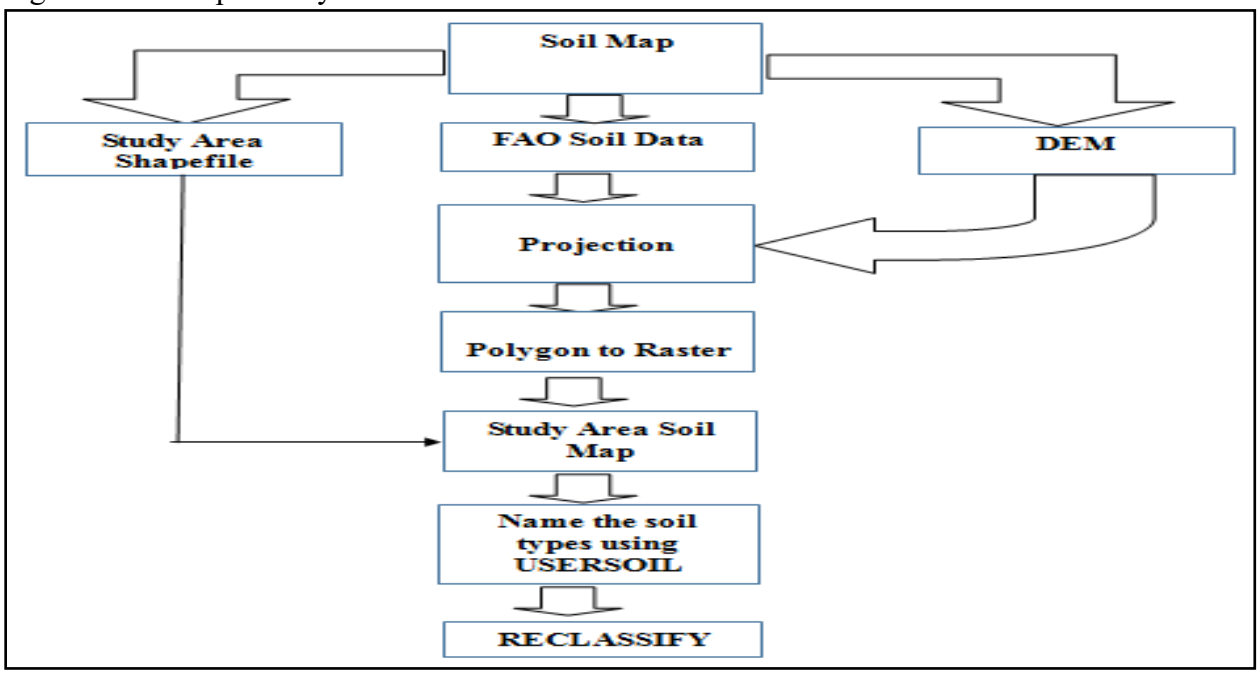

Figure 2: Schematic for generating soil map

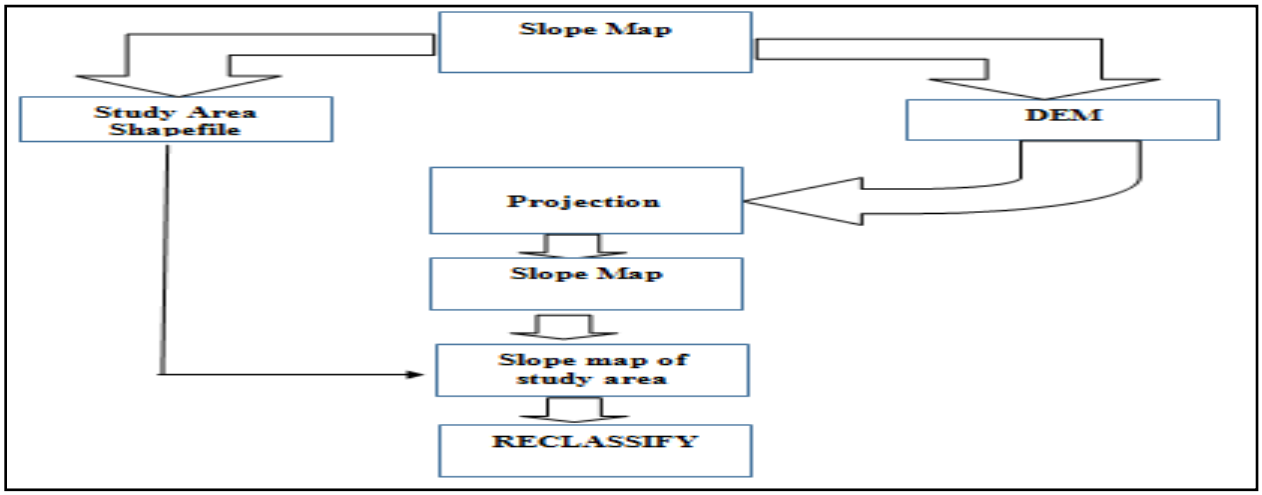

Figure 3: Schematic for generating slope map

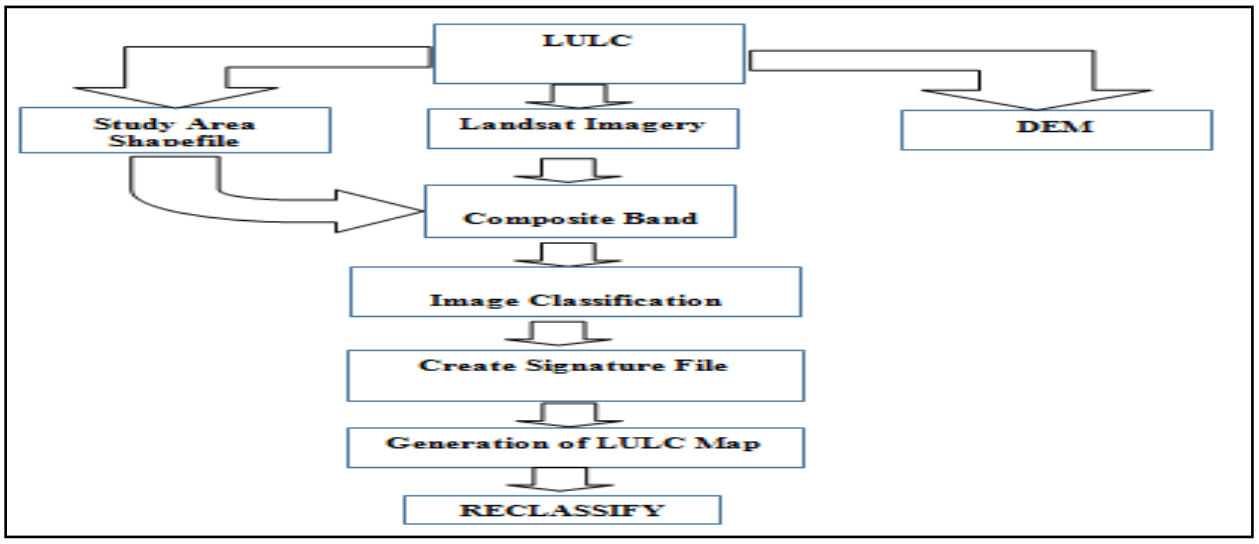

Figure 4: Schematic for generating land use land cover map

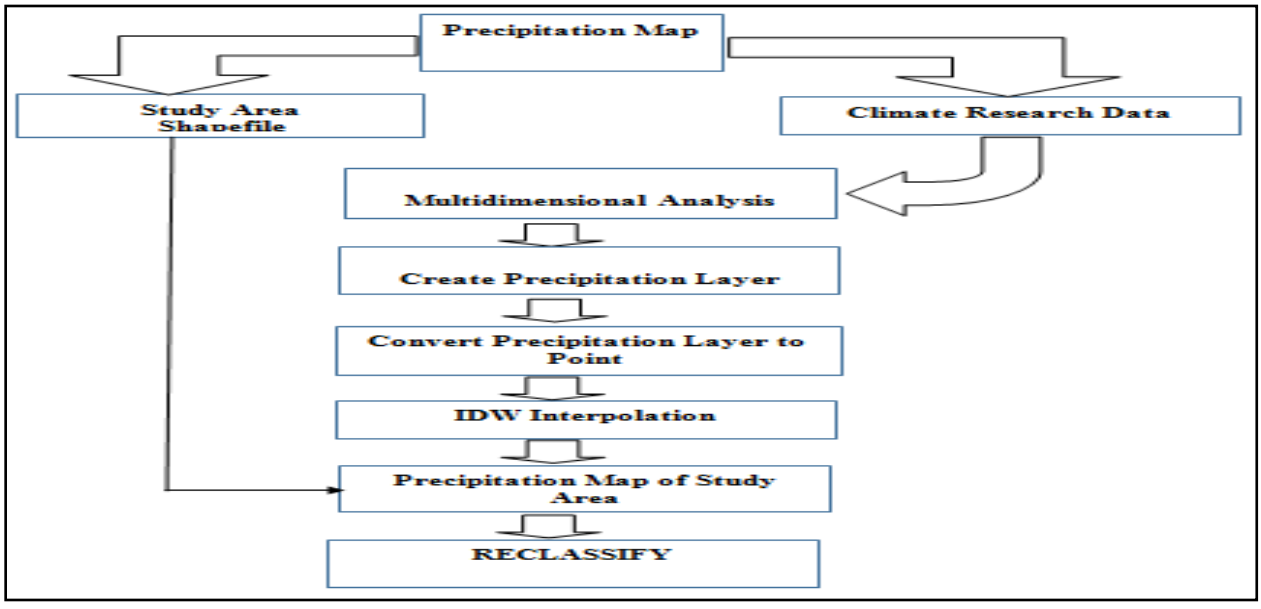

Figure 5: Schematic for generating precipitation map

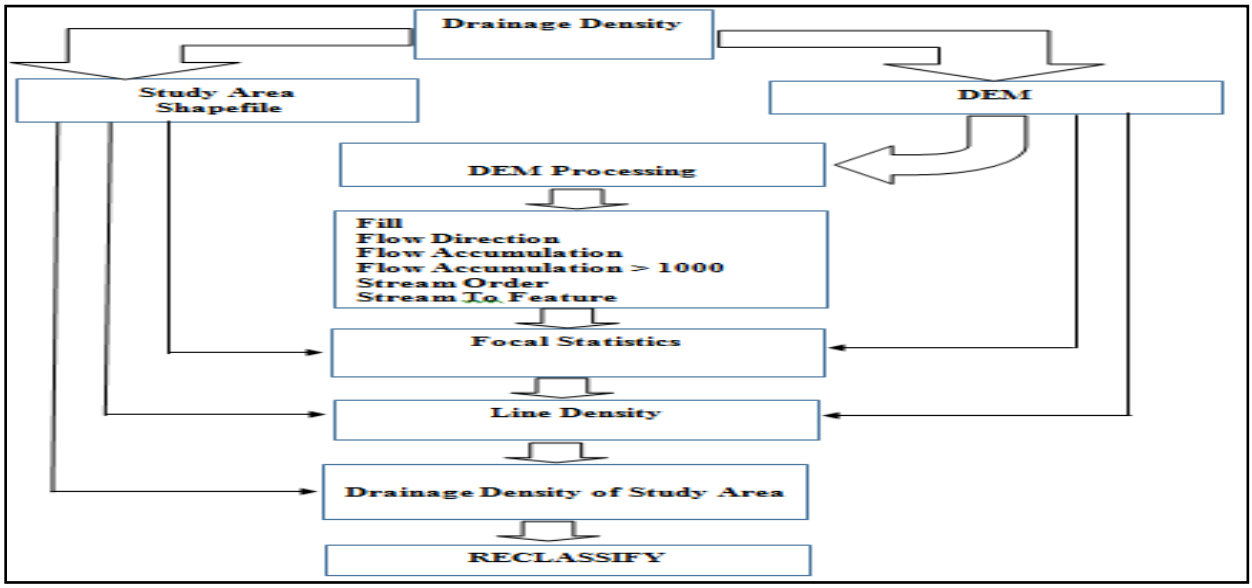

Figure 6: Schematic for generating drainage density map

2.6 Estimation of the Weight of Influence of Thematic Data using AHP

The weight of influence for each factor was computed statistically using analytical hierarchy process (AHP). The first step in obtaining the AHP design is to define the criteria and the sub-criteria. To define the one to nine scale of parameter significance, the scheme proposed by Saaty, reported in Table 2 was employed to translate linguistic judgments into numbers.

Table 2: Saaty summary table

Sig. Strength	Explanation	Comments
1	Equal significance	Two elements contribute equally to the objective
3	Moderate significance	Judgment slightly favours one element over another
5	Strong significance	Judgment strongly favours one element over another
7	Very strong significance	Judgment strongly favours one element over another, its dominance is demonstrated by experience
9	Maximum significance	The dominance of one element over another is demonstrated and absolute
2, 4, 6, 8	Can be used to express intermediate values	

To validate the AHP results, the index of consistency was employed. The principal eigenvalue (λ_{max}) is a function of the matrix divergence from consistency. In other words, a pairwise matrix is considered consistent only when λ_{max} equal or more than the number of the layers examined. The index of consistency was estimated using the mass balance equation of the form

$$CI = \frac{l_{max} - n}{n - 1} \quad (2.1)$$

Where; λ_{max} denotes the principal eigenvalue, and n represent the number of parameters. For a 3 by 3 matrix, the consistency index is less than 0.05. For a 4 by 4 matrix, it is 0.09 while for large

matrices, it is 0.1. If it matches, then the pairwise comparison is said to be consistent and the calculated weight of influence is said to be valid [27, 28].

3. Results and Discussion

The digital elevation model (DEM) and the reclassified DEM of the study area is presented in Figures 7 and 8 respectively.

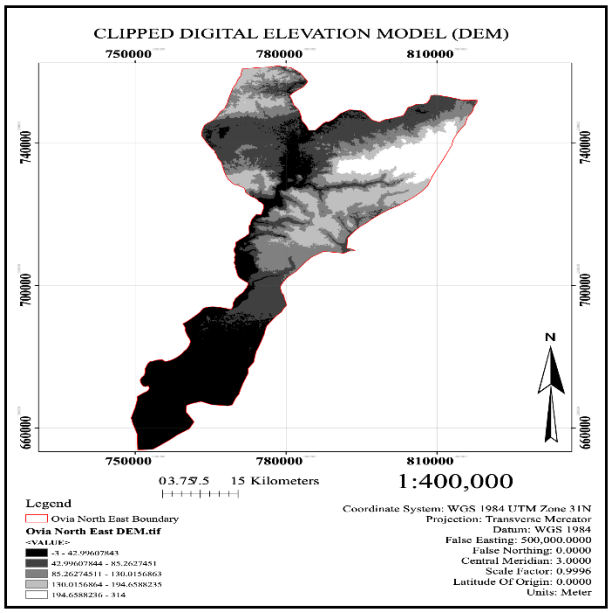

Figure 7: DEM of the study area

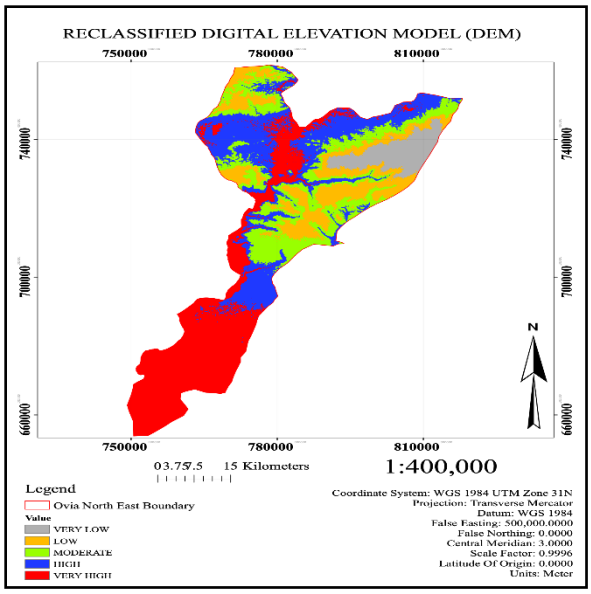

Figure 8: Reclassified DEM of the study area

Digital Elevation Models (DEMs) are integral to flood mapping due to their provision of detailed elevation and terrain data, facilitating the analysis of water flow paths during flood events, delineation of watersheds and drainage networks, and hydraulic modeling for predicting flood extents, depths, and velocities. By utilizing DEMs, hydrologists and engineers can accurately assess flood vulnerability, identify at-risk areas, and develop effective flood hazard maps for informed decision-making and risk mitigation strategies.

The slope map of the study area is presented in Figure 9a while the reclassified slope map is presented in Figure 9b

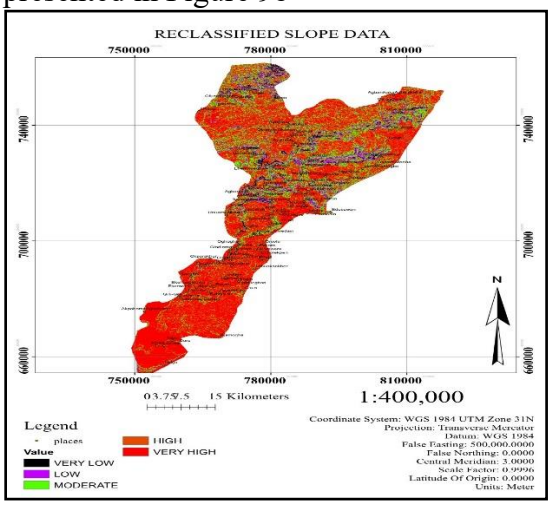

Figure 9a: Slope map of the study area

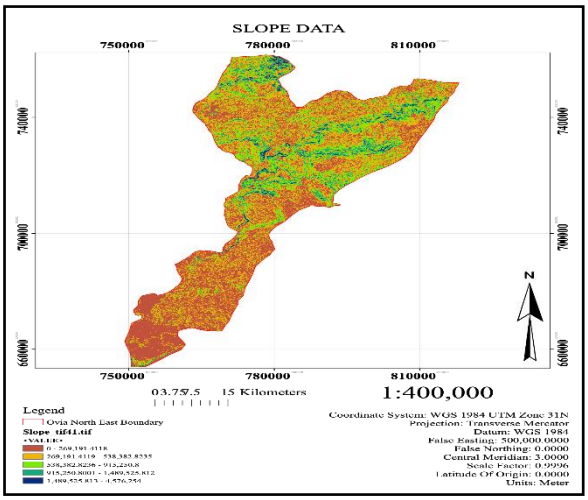

Figure 9b: Reclassified slope map

Elevation and slope significantly influence the stability of terrain, impacting surface runoff, subsurface drainage, and the direction of water flow. Slope plays a crucial role in determining the amount of rainfall contributing to streamflow, controlling overland flow duration, infiltration rates, and subsurface flow patterns. The combination of slope angles dictates the shape of the terrain and its relationship with soil type, drainage, lithology, and structure. Flooding can occur on both smooth and flat surfaces, facilitating fast water movement, while rougher surfaces can mitigate flood responses. Steeper slopes are more prone to surface runoff, while flat lands are susceptible to waterlogging. Low-gradient slopes are particularly sensitive to floods, as they tend to accumulate rainwater or excess river flow. Conversely, areas with steep slope gradients typically avoid flooding due to minimal water accumulation. The reclassified slope data shows a significant prevalence of high and very high slope areas, indicating regions with rapid water runoff potential. This finding is consistent with the study by Bui et al. (2019), which also identified steep slopes as a major factor in increasing flood susceptibility in the mountainous regions of Central Vietnam. Similarly, the research by Tehrany et al. (2015) in Malaysia highlighted that areas with steep slopes have a higher likelihood of experiencing flash floods due to the quick accumulation and movement of surface water. Both studies corroborate your findings that slope is a critical determinant of flood risk, reinforcing the notion that areas with higher slopes require targeted flood mitigation strategies. By aligning your results with these established studies, it becomes evident that your methodology and outcomes are in line with broader research trends, underscoring the validity of your flood risk assessment approach.

The soil map of the study area is presented in Figure 10a while the reclassified soil map is presented in Figure 10b

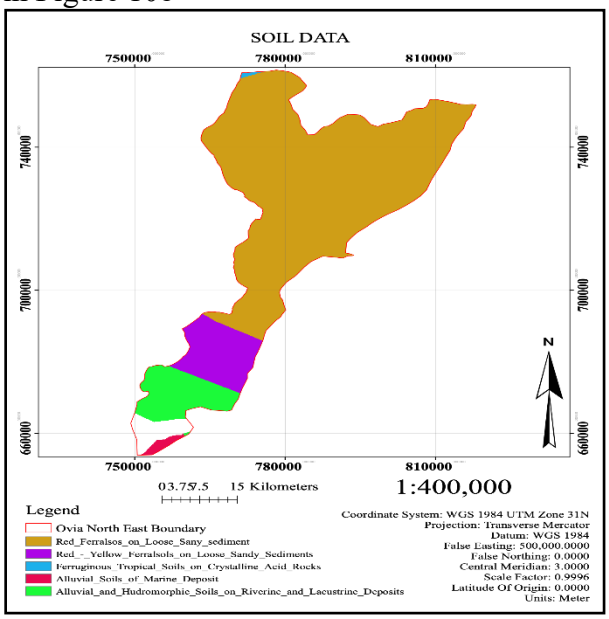

Figure 10a: soil map of the study area

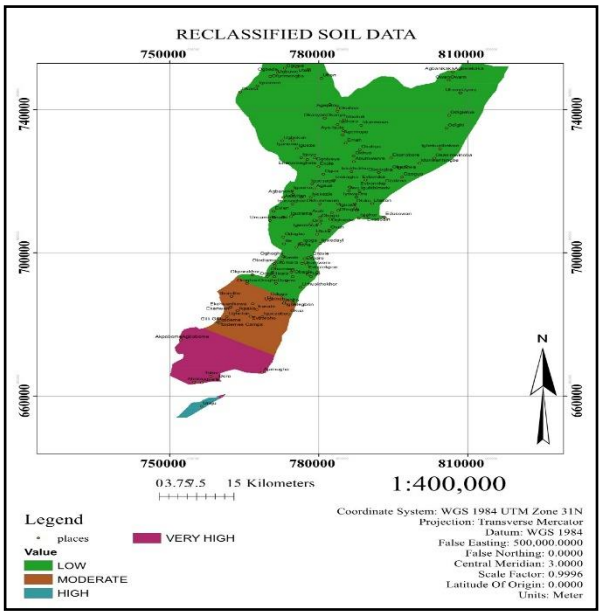

Figure 10b: Reclassified soil map

Soil texture and moisture content are pivotal characteristics influencing flooding dynamics. Sandy soils, with their high permeability, facilitate rapid water absorption and limited drainage, impacting flood susceptibility. Conversely, clay soils, less porous and retaining water for extended periods, are more prone to flooding. In the absence of data, soil moisture can be approximated through visual and tactile assessments, serving as the interface between land surface and atmosphere, crucial for runoff and groundwater storage from precipitation. Rainfall augments soil moisture, vital for erosion prevention, slope stability, and agricultural productivity. The soil's structural

composition and infiltration rate significantly influence its ability to absorb water, impacting flood risk. Soil type delineates its water entry capacity, affecting runoff rates. Flood vulnerability increases with diminished soil infiltration capacity, leading to heightened surface runoff and subsequent flooding when water input surpasses soil infiltration rates. In this study, the soil map was stratified based on infiltration capacity into highly, moderately, and less infiltrated soil categories, reflecting the municipality's diverse soil types. The majority of the research area comprises clay-loam soils, as indicated by the soil data classified into five infiltration classes. These classes were used to generate raster data groups, with each soil class weighted to construct a weighted soil map, facilitating the identification of areas with varying flood susceptibility based on soil characteristics

The soil land use land cover map of the study area is presented in Figure 11a while the reclassified land use land map is presented in Figure 11b

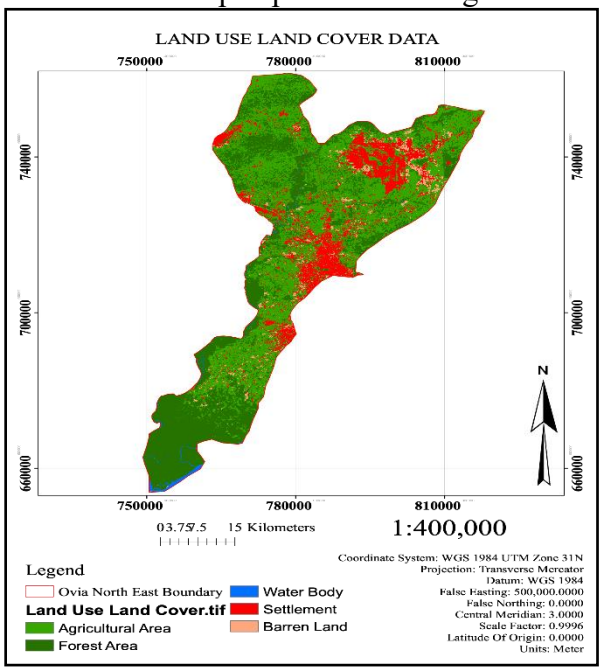

Figure 11a: LULC map of the study area

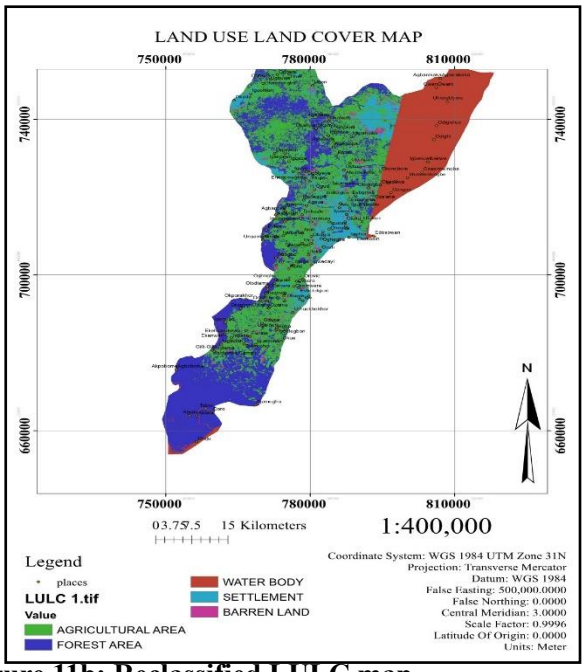

Figure 11b: Reclassified LULC map

Land use and land cover management play a central role in flood hazard mapping, as they reflect the current land utilization patterns, their spatial distribution, and their impact on soil stability and infiltration capacity. The vegetation cover, whether permanent grassland or other crops, influences the soil's ability to retain water, with bare fields exhibiting higher rates of rainwater runoff compared to fields with dense crop cover. Dense vegetation reduces runoff by slowing down the movement of water from the atmosphere to the soil surface. Conversely, impermeable surfaces such as concrete impede water absorption. Land use features such as buildings, roads, and urban areas decrease soil water retention capacity and increase surface runoff, often leading to accelerated flood peaks. Hence, land use types act as water-resistant surfaces, accelerating water accumulation and exacerbating flood severity. Municipal zoning maps were utilized to delineate land use and land cover classes within the study area, providing essential data for flood risk assessment and management

The drainage density map of the study area is presented in Figure 12a while the reclassified drainage density map is presented in Figure 12b

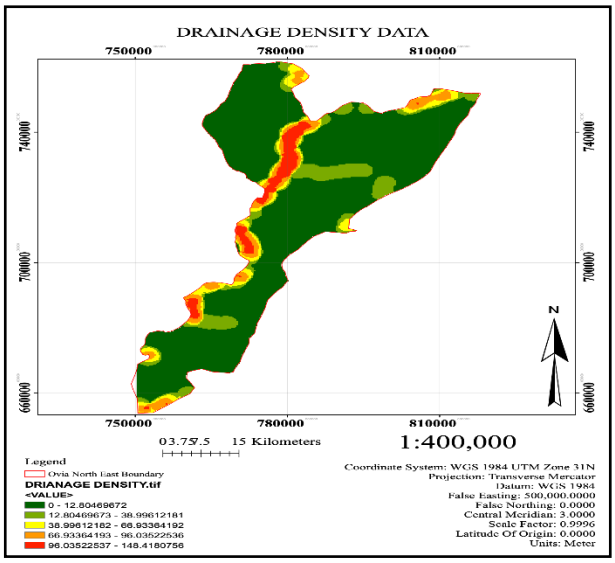

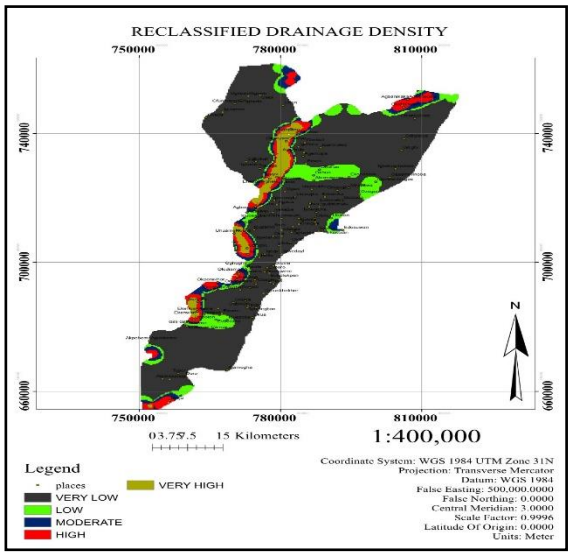

Figure 12a: Drainage density map of the study area **Figure 12b: Reclassified drainage density map**

Drainage systems are integral ecosystems for mitigating risks, as they provide insights into soil characteristics and geotechnical properties, indicating vulnerability to erosion and sedimentation in regions with higher population densities. Quantitative hazard analysis commences with stream order assignment, following the Strahler method (1964), which organizes streams based on their hierarchical structure. Utilizing this method, a drainage density map is generated, depicting the ratio of total stream length to watershed area. The calculation of drainage density (D = L / A) involves the length of drainage channels (L) in kilometers within the watershed and the total area of the watershed (A) in square kilometers. Watersheds are classified based on drainage density, with classes ranging from 1 to 5, where moderate to subpar watersheds fall within the 1-5 range, while those with efficient drainage exhibit values below 5. In the study area, second-order streams were identified, with the primary river, Ogbese River, coursing through settlements in Ovia North-East, illustrating an accumulation of flow. The drainage density layer was further categorized into five sub-groups using standard schemes, assigning values ranging from 1 (extremely high drainage density) to 5 (extremely low drainage density).

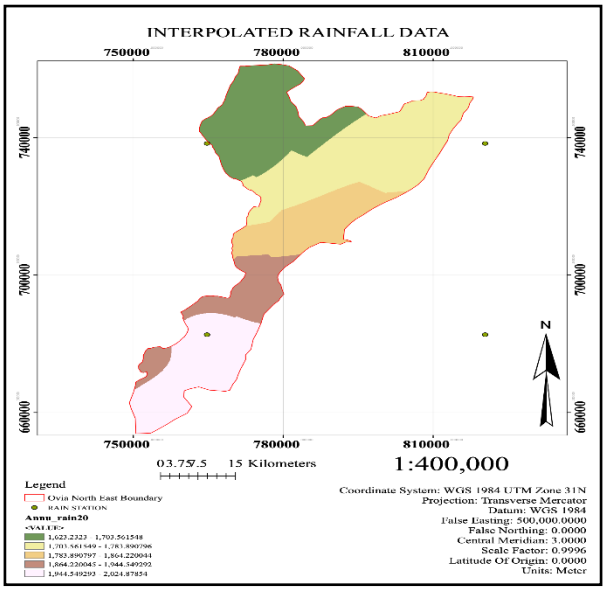

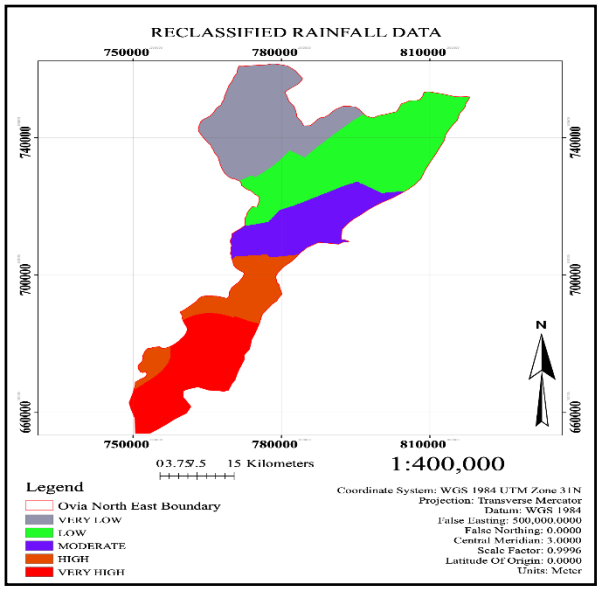

Figure 13a: Drainage density map of the study area **Figure 13b: Reclassified drainage density map**

The precipitation map of the study area is presented in Figure 13a while the reclassified precipitation map is presented in Figure 13b

Various factors, including prolonged periods of heavy precipitation, can lead to flooding. Heavy rainfall often overwhelms natural watercourses, preventing them from adequately channeling the excess water. Floods are primarily triggered by extreme rainfall events, with any surplus water not absorbed by the ground flowing downhill as runoff. The volume of runoff varies depending on the intensity of rainfall in a given area, leading to increased water levels in rivers and lakes. Riverine floods occur when water levels exceed the capacity of river banks or dams, resulting in overflow onto adjacent areas. While local rainfall is a key factor in pluvial flooding, the study highlights the significance of rainfall amounts in upstream catchments, which also contribute to the risk of river-induced flooding. Given the modest size of the research area, both local and upstream rainfall data were incorporated into the analysis. The resulting raster layer was classified into five classes using equal intervals, with each class assigned a number from 1 to 5, representing increasing levels of precipitation, ranging from the least (1) to the greatest (5). The flood map was generated using weighted overlay. The estimated weight of influence of the different thematic data from the AHP analysis is presented in Table 3

Table 3.7: Estimated weight of influence of the different

Parameter	Relative Weight (%)	Reclassified Parameter	Ranking
Rainfall (mm)	19	1,842.976196 - 1,902.241461 1,902.241462 - 1,947.764055 1,947.764056 - 1,991.568816 1,991.568817 - 2,031.937909 2,031.93791 - 2,062	1 2 3 4 5
Drainage density (km/km^2)	18	0 - 19.88931239 19.8893124 - 60.4966585 60.49665851 - 101.932726 101.9327261 - 142.5400721 142.5400722 - 211.3239441	1 2 3 4 5
Elevation (meters)	13	-2 - 28.77254902 28.77254903 - 45.98431373 45.98431374 - 65.80392157 65.80392158 - 91.88235294 91.88235295 – 131	5 4 3 2 1
Slope (degrees)	16	0 - 193,907.8588 193,907.8589 - 430,906.3529 430,906.353 - 840,267.3882 840,267.3883 - 1,939,078.588 1,939,078.589 - 5,494,056	5 4 3 2 1
Soil classes	17	1373 5746 19599	4 3 2

Urban land-use	17	Vegetation Barren Land Settlement Agricultural Area Water Body	1 2 3 4 5

A consistency Index (CI) of 0.046 and a Random Index (RI) for 6 (Six) parameter computations yielded a final value of 1.24. The maximum permitted values for CI and RI are 0.1 and 10%, respectively. With an estimated index of consistency of 0.046, it was concluded that the pairwise comparison is consistent and the calculated weight of influence is valid. Hence, the final flood vulnerability map was generated using weighted overlay and result is presented in Figure 14

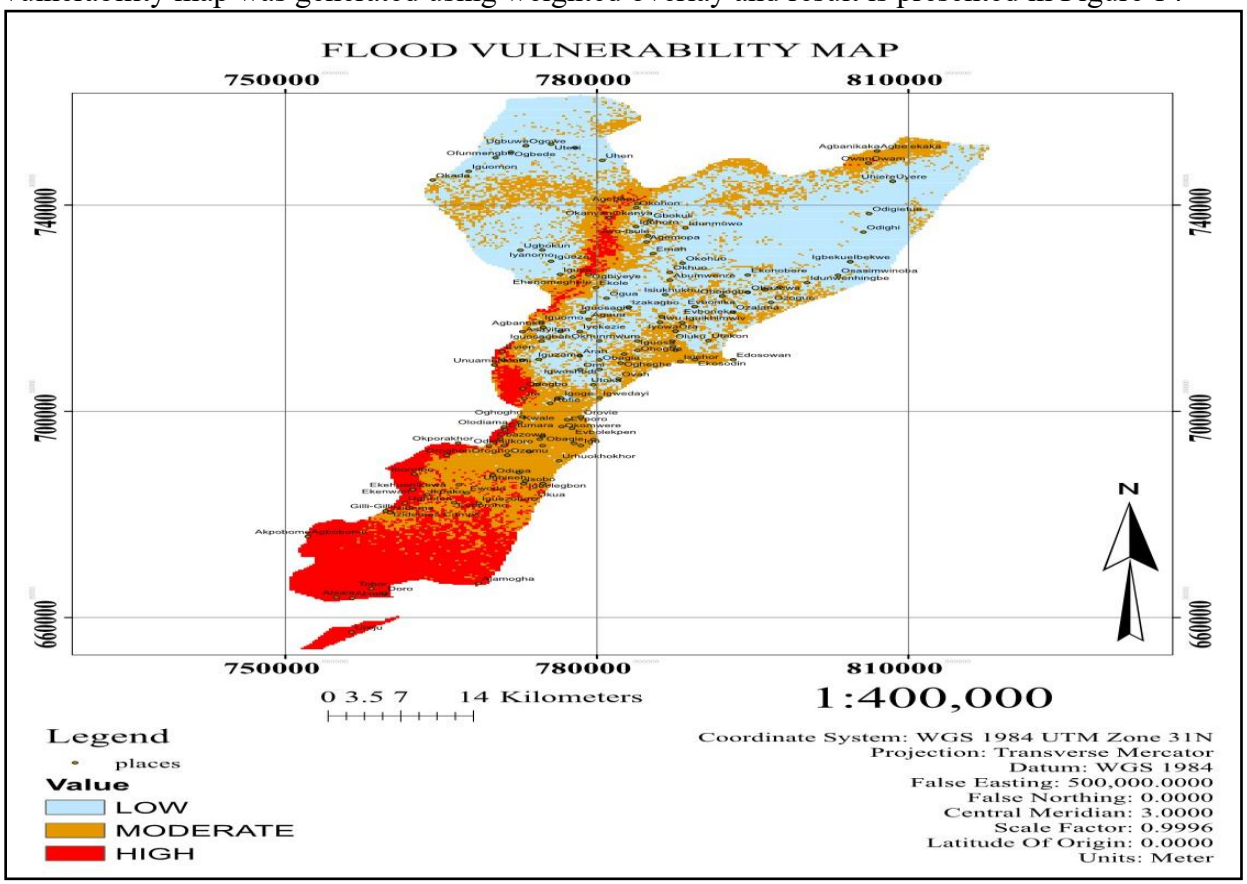

Figure 14: **Final Flood Map of the Study Area**

4. Conclusion

From the final flood map, it was observed that majority of the study area – roughly 24 percent, or 46823.878sqm. - is a high flood vulnerable area while 24 percent of the study area is moderately vulnerable and 52 per cent of the study area has a low vulnerability. The beauty of a flood map lies in its potential to identify communities that are at the risk of flood event. From the flood map generated in this study, it was observed that communities such as Abiala, Agbobome, Ago-Iredia, Ajamogha, Akpobome, Doro, Egbatan, Ekehuan, Evbuerebor, Evien, Gilli-Gilli, Iboro, Iguohemwen, Ikewa, Isobo, Izideme, Odogbo, Oduna, Olodiama, Oroghon, Otumara, Owam, Tobor, Ughoton, Unuame and Ureju are highly sensitive flood-prone areas. Communities such as; Agbelekaka, Agbonmoba, Agemopa, Agepanu, Ago Erierie, Akhuakhuari, Ehenomeghele,

Ekiadolor, Ekole, Ekosodin, Emianghan, Evbolekpen, Evboroho, Evporo, Ewode, Idunmwowina, Igbobi, Igo, Igoge, Iguelegbon, Iguezoba, Iguikhimwiv, Iguiodia, Iguomo, Iguosa, Iguosagie, Iguosodin, Iguosula, Igwedayi, Igwoshodi, Ikiadolor, Ikoro, Ikpako, Isiehor, Ite, Iwu, Iyowa, Kwale, Obagie, Obarenren, Obazuwa, Obojogbo, Odighi, Ogbiyeye, Ogbogiobo, Oghede, Ogheghe, Oghogho, Okada, Okanyan, Okhunmwum, Okohon, Okomwere, Okporoma, Okua, Oluku, Olumoye, Ora, Orogho, Ozalana, Ozomu, Rofie, Sobetie, Ugbineh, and Urhuokhokhor are moderately vulnerable to flooding. Other communities such as; Abumwenre, Adeyanba, Agaua, Agbanoko, Agbonmoba, Aihuobabekun, Arah, Awiwabekun, Ayo-Isule, Egbeta, Ekonobore, Emah, Evboneka, Gbokuli, Ibekwe, Idunmowo, Idunwenhingbe, Igbekue, Iguadolor, Igueze, Iguhoro, Iguomon, Iguosagban, Iguoshodi Nebudin, Iguye, Iguzama, Isiukhukhu, Iyanomo, Iyekezie, Izakagbo, Obagia, Odighi, Odigietue, Ofunmengbe, Ogbede, Ogowe, Ogua, Ohogua, Okabeghe, Okohuo, Old Iyekezie, Omi, Orovie, Osasimwinoba, Ovah, Ozoguo, Ugbokun, Ugbuwe, Uhen, Uhiere, Utekon, Utesi, Utoka, and Uyere are located in low flood vulnerable zones. Finally, the three main causes of flooding in the study area are land cover change, severe rainfall, and a high drainage density of 0.087m/m^2. Land subsidence is another factor that increases future flood risk.

References

[1] Nasiri, H., Mohd, J.M.Y., Thamer, A.M.A. (2016). An overview to flood vulnerability assessment methods. *Sustainable Water Resources Management*, 2, 331–336.
[2] Sarkar, D., Mondal, P. (2020). Flood vulnerability mapping using frequency ratio (FR) model: a case study on Kulik river basin, Indo-Bangladesh Barind region. *Applied Water Science*, 10(1), 17.
[3] Erena, S.H., Worku, H. (2018). Flood risk analysis: causes and landscape-based mitigation strategies in Dire Dawa city, Ethiopia. *Geoenvironmental Disasters*, 5(1), 16.
[4] Ali, S.A., Khatun, R., Ahmad, A., Ahmad, S.N. (2019). Application of GIS based analytic hierarchy process and frequency ratio model to flood vulnerable mapping and risk area estimation at Sundarban region, India. *Modeling Earth Systems and Environment*, 5(3), 1083–1102.
[5] Indrayani, P., Mitani, Y., Djamaluddin, I., Ikemi, H. (2018). Spatial-temporal vulnerability and risk assessment model for urban flood scenario. *ASM Science Journal*, 11(Special Issue 3), 233–245.
[6] Panhalkar, S.S., Jarag, A.P. (2017). Flood risk assessment of Panchganga River (Kolhapur district, Maharashtra) using GIS-based multicriteria decision technique. *Current Science*, 112(4), 785.
[7] Wei, C., Haoyuan, H., Shaojun, L., Himan, S., Yi, W., Xiaojing, W., Baharin, B.A. (2019). Flood susceptibility modelling using novel hybrid approach of reduced-error pruning trees with bagging and random subspace ensembles. *Journal of Hydrology*, 575, 864–873.
[8] Hong, H., Panahi, M., Shirzadi, A., Ma, T., Liu, J., Zhu, A.X., Chen, W., Kougias, I., Kazakis, N. (2018). Flood susceptibility assessment in Hengfeng area coupling adaptive neuro-fuzzy inference system with genetic algorithm and differential evolution. *Science of the Total Environment*, 621, 1124–1141.
[9] Cao, C., Xu, P., Wang, Y., Chen, J., Zheng, L., Niu, C. (2016). Flash Flood Hazard Susceptibility Mapping Using Frequency Ratio and Statistical Index Methods in Coalmine Subsidence Areas. *Sustainability*, 8, 948.
[10] Pilon, P.J. (Ed.). (2004). *Guidelines for reducing flood losses*. New York: ISDR.
[11] Wisner, B., Blaikie, P., Cannon, T., Davis, I. (2004). *At risk: Natural hazards, people's vulnerability and disasters*. New York: Routledge.
[12] Sofia, G., Roder, G., Dalla Fontana, G., Tarolli, P. (2017). Flood dynamics in urbanized landscapes: 100 years of climate and human's interaction. *Scientific Reports*, 7, 40527.

[13] Alho, P., Sane, M., Huokuna, M., Käyhkö, J., Lotsari, E., Lehtiö, L. (2008). Mapping of floods. *Environmental Administration Guidelines*, 2, 59-101.
[14] Izinyon, O.C. (2018). Flood Hazard Modelling and Management. A paper presented in one of the technical sections of the Nigeria Society of Engineers, 1-16.
[15] Klijn, F. (2009). *Flood risk assessment and flood risk management: An introduction and guidance based on experience and findings of FLOOD site (an EU-funded Integrated Project)*. Delft: Deltares, Delft Hydraulics.
[16] Ehiorobo, J.O., Izinyon, O.C., Ilaboya, I.R. (2012). Effects of Climate Change on River flow regimes in the Mangrove and Tropical Rain Forest Region of West Africa. Presented at an International Workshop on Exchange of Experience in Water Resources Management Between Europe/China/Africa/Latin America, 15–18 October, 2012. Organized by European Commission Joint Research Centre, ISPRA, Italy.
[17] Kundzewicz, Z.W., Piniewski, M., Mezghani, A., Okruszko, T., Pińskwar, I., Kardel, I. (2018). Assessment of climate change and associated impact on selected sectors in Poland. *Acta Geophysica*, 66(6), 1509–1523.
[18] Bloschl, G., Hall, J., Parajka, J., Perdigao, R.A.P., Merz, B., Arheimer, B., Aronica, G.T., Bilibashi, A., Bonacci, O., Borga, M. (2017). Changing climate shifts timing of European floods. *Science*, 357, 588–590.
[19] Gebrehiwot, A.A., Hashemi-Beni, L. (2021). Three-dimensional inundation mapping using UAV image segmentation and digital surface model. *ISPRS International Journal of Geo-Information*, 10, 144.
[20] ISDR (International Strategy for Disaster Reduction). (2004). *Living with risk: A global review of disaster reduction initiatives*. Geneva: ISDR.
[21] ISDR (International Strategy for Disaster Reduction). (2007). *Disaster risk reduction: A global review 2007*. Geneva: ISDR.
[22] Matej, V., Vojteková, J. (2019). Flood Susceptibility Mapping on a National Scale in Slovakia Using the Analytical Hierarchy Process. *Water*, 11(364), 1-17.
[23] Al Baky, M.A., Islam, M., Paul, S. (2019). Flood hazard, vulnerability and risk assessment for different land use classes using a flow model. *Earth Systems and Environment*, 4, 1–20.
[24] Hoque, M.A.-A., Tasfia, S., Ahmed, N., Pradhan, B. (2019). Assessing spatial flood vulnerability at Kalapara Upazila in Bangladesh using an analytic hierarchy process. *Sensors*, 19(6), 1302.
[25] Mundhe, N. (2019). Multi-criteria decision making for vulnerability mapping of flood hazard: a case study of Pune city. *Journal of Geographical Studies*, 2(1), 41–52.
[26] Cafiero, C., Vakis, R.N. (2006). Risk and vulnerability considerations in poverty analysis: recent advances and future directions. *World Bank, Social Protection*, Washington.
[27] Singh, L.K., Jha, M.K., and Chowdary, V.M. (2017). Multi-criteria analysis and GIS modeling for identifying prospective water harvesting and artificial recharge sites for sustainable water supply, J. Clean. Prod., 142, 1436–1456
[28] Saaty T. L. (1980), The Analytic Hierarchy Process, McGraw-Hill, New York., 67-78
[29] Bui, D.T., Shahabi, H., Alizadeh, M., Ahmad, B.B., Samui, P., Ho, L.S., & Panahi, M. (2019). Spatial prediction of rainfall-induced landslides using a hybrid machine learning approach based on Random Subspace and Classification and Regression Trees. *CATENA*, 175, 203-213. DOI: 10.1016/j.catena.2018.12.018.
[30] Tehrany, M.S., Pradhan, B., & Jebur, M.N. (2015). Flood susceptibility mapping using GIS-based support vector machine and frequency ratio models in Tehran province, Iran. *Journal of Hydrology*, 528, 240-252. DOI: 10.1016/j.jhydrol.2015.06.028